

Mechanistic Studies of Nitric Oxide Reactions with Water Soluble Iron(II), Cobalt(II), and Iron(III) Porphyrin Complexes in Aqueous Solutions: Implications for Biological Activity

Leroy E. Laverman¹ and Peter C. Ford*

Contribution from the Department of Chemistry and Biochemistry, University of California, Santa Barbara, California 93106

Received June 6, 2001

Abstract: The reactions of nitric oxide and carbon monoxide with water soluble iron and cobalt porphyrin complexes were investigated over the temperature range 298–318 K and the hydrostatic pressure range 0.1–250 MPa [porphyrin ligands: TPPS = tetra-meso-(4-sulfonatophenyl)porphinate and TMPS = tetra-meso-(sulfonatesityl)porphinate]. Large and positive ΔS^\ddagger and ΔV^\ddagger values were observed for NO binding to and release from iron(III) complexes Fe^{III}(TPPS) and Fe^{III}(TMPS) consistent with a dissociative ligand exchange mechanism where the lability of coordinated water dominates the reactivity with NO. Small positive values for $\Delta S^\ddagger_{\text{on}}$ and $\Delta V^\ddagger_{\text{on}}$ for the fast reactions of NO with the iron(II) and cobalt(II) analogues ($k_{\text{on}} = 1.5 \times 10^9$ and $1.9 \times 10^9 \text{ M}^{-1} \text{ s}^{-1}$ for Fe^{II}(TPPS) and Co^{II}(TPPS), respectively) indicate a mechanism dominated by diffusion processes in these cases. However, reaction of CO with the Fe^{II} complexes ($k_{\text{on}} = 3.6 \times 10^7 \text{ M}^{-1} \text{ s}^{-1}$ for Fe^{II}(TPPS)) displays negative $\Delta S^\ddagger_{\text{on}}$ and $\Delta V^\ddagger_{\text{on}}$ values, consistent with a mechanism dominated by activation rather than diffusion terms. Measurements of NO dissociation rates from Fe^{II}(TPPS)(NO) and Co^{II}(TPPS)(NO) by trapping free NO gave k_{off} values of $6.3 \times 10^{-4} \text{ s}^{-1}$ and $1.5 \times 10^{-4} \text{ s}^{-1}$. The respective M^{II}(TPPS)(NO) formation constants calculated from $k_{\text{on}}/k_{\text{off}}$ ratios were 2.4×10^{12} and $1.3 \times 10^{13} \text{ M}^{-1}$, many orders of magnitude larger than that ($1.1 \times 10^3 \text{ M}^{-1}$) for the reaction of Fe^{III}(TPPS) with NO.

Introduction

Nitric oxide (nitrogen monoxide) has significant roles in mammalian biology as an intracellular signaling agent and in cytotoxic immune response.² The principal targets for NO under bioregulatory conditions are metal centers, primarily iron.³ Although the ferro-heme enzyme soluble guanylyl cyclase (sGC) is the best characterized example,⁴ various reports point to roles in inhibition of metalloenzymes such as cytochrome oxidase,⁵ nitrile hydratase,⁶ and catalase⁷ and in vasodilator properties of nitrophorins, a class of ferri-heme proteins found in certain blood sucking insects.⁸ Concentrations of NO generated for bioregulation are low ([NO] < 1 μM reported in endothelium cells for blood pressure control).⁹ Thus, reactions with targets as

sGC necessarily have very high rate constants (k_{on}) to compete effectively with other physical and chemical processes leading to NO depletion.

Clearly, understanding the interaction between NO and metal targets is key to understanding the *in vivo* chemistry of nitric oxide.¹⁰ An important question to address is whether the free radical nature of NO affects the dynamics of NO substitution reactions on metal centers or whether NO behaves in a manner more similar to other Lewis bases. It is with such questions in mind that the present investigation of NO reactions with water soluble ferri- and ferro-heme porphyrins was undertaken.

Rates of NO reactions with heme centers have been studied previously by laser flash photolysis techniques, where NO is photolabilized from a M–NO precursor and subsequent relaxation to equilibrium is followed spectroscopically.^{10,11} Indeed reactions of NO with heme centers were investigated long before the bioregulatory functions of NO were postulated.¹⁰ Despite

(1) Taken in part from: Laverman, L. E. Ph.D. Dissertation, University of California, Santa Barbara, CA, 1999.

(2) (a) Moncada, S.; Palmer, R. M. J.; Higgs, E. A. *Pharmacol. Rev.* **1991**, *43*, 109–142. (b) Feldman, P. L.; Griffith, O. W.; Struehr, D. J. *Chem. Eng. News* **1993**, *71*, 10, 26–38.

(3) (a) Radi, R. *Chem. Res. Toxicol.* **1996**, *9*, 828–835. (b) Traylor, T.; Sharma, V. S. *Biochemistry* **1992**, *31*, 2847–2849.

(4) Kim, S.; Deinum, G.; Gardner, M. T.; Marletta, M. M.; Babcock, G. T. *J. Am. Chem. Soc.* **1996**, *118*, 8769–8770 and references therein.

(5) Cleeter, M. W. J.; Cooper, J. M.; Darley-Usmar, V. M.; Moncada, S.; Scapira, A. H. V. *FEBS Lett.* **1994**, *345*, 50–54.

(6) Noguchi, T.; Honda, J.; Nagamune, T.; Sasabe, H.; Inoue, Y.; Endo, I. *FEBS Lett.* **1995**, *358*, 9–12.

(7) Brown, G. E. *Eur. J. Biochem.* **1995**, *232*, 188–191.

(8) Ribiero, J. M. C.; Hazzard, J. M. H.; Nussenzveig, R. H.; Champagne, D. E.; Walker, F. A. *Science* **1993**, *260*, 539–541.

(9) Malinski, T.; Czuchajowski, C. In *Methods in Nitric Oxide Research*; Feelish, M., Stamler, J. S., Eds.; J. Wiley and Sons: Chichester, U.K., 1996; Chapter 6 and references therein.

(10) (a) Gordunov, N. V.; Osipov, A. N.; Day, W. B.; Zayas-River, B.; Kagan, V. E.; Elsayed, N. M. *Biochemistry* **1995**, *34*, 6689–6699. (b) Yoshimura, T.; Iwasaki, H.; Shidara, S.; Suzuki, S.; Nakahara, A.; Matsubara, T. *J. Biochem. (Tokyo)* **1988**, *103*, 1016–1019. (c) Stochel, G.; Ilkowska, E.; Pawelec, M.; Wanat, A.; Wolak, M. *ACH—Models Chem.* **1998**, *135*, 847–871. (d) Morse, R. H.; Chan, S. J. *J. Biol. Chem.* **1980**, *255*, 7876–7882. (e) Henry, Y.; Banerjee, R. J. *Mol. Biol.* **1973**, *73*, 469–482. (f) Brudvig, G. W.; Stevens, T. H.; Chan, S. J. *Biochemistry* **1980**, *19*, 5275–5285. (g) Petrich, J. W.; Poyart, C.; Martin, J. L. *Biochemistry* **1988**, *27*, 4049. (h) Antonini, E.; Brunori, M. *Hemoglobin and Myoglobin in Their Reactions with Ligands*; North-Holland Publishing Co.: Amsterdam, 1971. (i) Duprat, A. F.; Traylor, T. G.; Wu, G.-Z.; Coletta, M.; Sharma, V. S.; Walda, K. N.; Magde, D. *Biochemistry* **1995**, *34*, 2634–2644. (j) Bohle, D. S.; Hung, Ch.-H. *J. Am. Chem. Soc.* **1995**, *117*, 9584–9585.

this research activity, the mechanisms by which NO reacts with heme iron, that is, the “on” reaction for eq 1, (Por = porphyrin moiety), have only recently been systematically probed.



Reported here are the activation parameters ΔH^\ddagger , ΔS^\ddagger , and ΔV^\ddagger determined from the temperature (T) and hydrostatic pressure (P) effects on the reactions of NO with the iron(III) and iron(II) analogues of Fe(TPPS) (**Ia** and **Ib**) and Fe(TMPS) (**IIa** and **IIb**) [TPPS = tetrameso(4-sulfonatophenyl) porphinate; TMPS = tetrameso(sulfonatomesityl) porphinate] in aqueous solution. Also described are the activation parameters ΔH^\ddagger and ΔS^\ddagger determined for Co^{II}(TPPS). The activation parameters lend insight into the reaction mechanism(s) for the “on” and “off” processes, and these data for the model systems will be compared with similar data for reactions of met-myoglobin (mMb).¹² Aspects of this work have been reported in preliminary communications.¹³

Experimental Section

Materials. All materials were used as received unless otherwise stated. Nitric oxide was purchased from Matheson Gas Co. and passed through KOH pellets to remove higher nitrogen oxides and through a water scrubbing column prior to use. Nitric oxide concentrations were calculated using solubility data from Battino.¹⁴ Carbon monoxide was purchased from Matheson Gas Co. and passed through an oxygen scrubbing column prior to addition to aqueous samples using vacuum line techniques. CO concentrations were calculated using published data.¹⁵ Fe^{III}(TPPS) (**Ia**) and Co^{III}(TPPS) (**IIIa**) were purchased from MidCentury Chemicals. Synthesis of Fe^{III}(TMPS) (**IIa**) was performed by a modification of the procedure described by Cheng.¹⁶

Solution Preparation. Samples of **Ia** and **IIa** for spectroscopic studies were prepared by dissolving the compound in deionized water made acidic by addition of one drop of 1 M HCl to ~100 mL of solution followed by several freeze pump thaw (fpt) cycles in a specially designed cuvette. In situ preparations of Fe^{II}(TPPS) (**Ib**) and Fe^{II}(TMPS) (**IIb**) were accomplished by addition of a slight excess of sodium dithionite to solutions of **Ia** and **IIa** in 50 mM pH 7.0 phosphate buffer under inert conditions. Solutions of Co^{III}(TPPS) in 50 mM pH 7.0 phosphate buffer undergo reductive nitrosylation in the presence of NO to give the Co^{II}(TPPS)(NO) (**IIIb**) analogue. Under NO ($P_{\text{NO}} = 1$ atm), this reaction was complete in 10–15 min at ambient temperatures. Solutions were exposed to the desired partial pressure of NO at the reaction temperature and allowed to equilibrate for a minimum of 15 min with periodic stirring. Solutions were equilibrated an additional 15 min in a temperature controlled cuvette holder on the laser flash photolysis system. Solutions for high-pressure laser flash photolysis were transferred via syringe into a cylindrical cuvette with a Teflon piston in an inert atmosphere box. The sliding piston allowed for transmission of hydrostatic pressures to the solution within the cuvette.

(11) (a) Hoshino, M.; Ozawa, K.; Seki, H.; Ford, P. C. *J. Am. Chem. Soc.* **1993**, *115*, 9568–9575. (b) Tamura, M.; Kobayashi, K.; Hayashi, K. *FEBS Lett.* **1978**, *88*, 124–126. (f) Rose, E. J.; Hoffman, B. *J. Am. Chem. Soc.* **1983**, *105*, 2866–2873. (c) Cornelius, P. A.; Hochstrasser, R. M.; Steele, A. W. *J. Mol. Biol.* **1983**, *163*, 119–128. (d) Jongeward, K. A.; Magde, D.; Taube, D. J.; Marsters, J. C.; Traylor, T. G.; Sharma, V. S. *J. Am. Chem. Soc.* **1988**, *110*, 380–387.

(12) Laverman, L. E.; Wanat, A.; Oszejca, J.; Stochel, G.; Ford, P. C.; van Eldik, R. *J. Am. Chem. Soc.* **2001**, *123*, 285–293.

(13) (a) Laverman, L. E.; Ford, P. C. *Chem. Commun.* **1999**, 1843–1844. (b) Laverman, L. E.; Hoshino, M.; Ford, P. C. *J. Am. Chem. Soc.* **1997**, *119*, 12663–12664.

(14) Battino, R. In *IUPAC Solubility Data Series: Oxides of Nitrogen*; Young, C. L., Ed.; Pergamon Press: Oxford, U.K., 1981; 260–261.

(15) *IUPAC Solubility Data Series: Carbon Monoxide*; Pergamon Press: Oxford, England, 1990; Vol. 43.

(16) Cheng, S.; Chen, Y.; Su, Y. O. *J. Chin. Chem. Soc.* **1991**, *38*, 15–22.

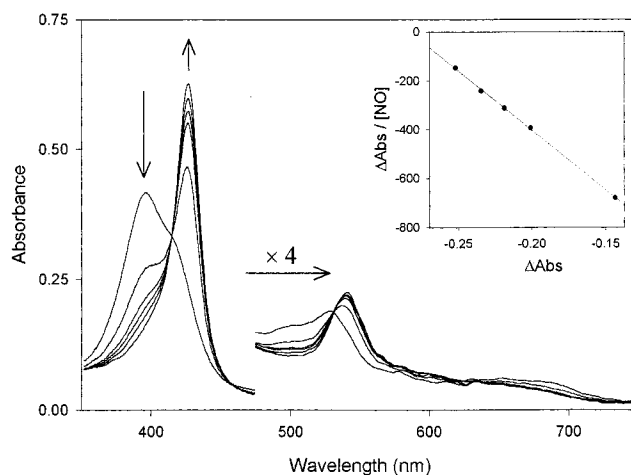


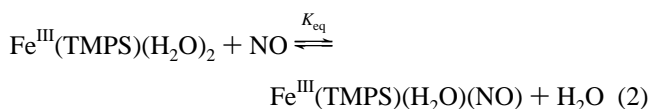
Figure 1. Spectral changes of Fe^{III}(TMPS) at 25 °C as a function of increasing [NO]. Inset: Scatchard plot at 396 nm, $K_{\text{eq}} = 4.85 \pm 0.1 \times 10^3 \text{ M}^{-1}$.

Laser Flash Photolysis. Temperature and pressure dependent laser flash photolysis kinetic studies were performed on a “pump–probe” system described previously.¹⁷ Excitation was at 355 nm, the third harmonic of a Nd:YAG laser (Continuum, NY61). The probe beam source was a xenon arc lamp that was channeled through monochromators before and after passing through the sample. Changes in transmitted light intensity were monitored by a photomultiplier tube (PMT) coupled to a digitizing oscilloscope (Tektronix, TDS 540), and data were transferred to a computer for subsequent kinetic analysis. Reported rate constants are the averages of several kinetic traces obtained by repeatedly averaging signals from individual relaxation profiles. Transient absorbance spectra were recorded by passing white light through the sample and into a gated CCD based spectrograph (Acton Research Corp., Princeton Applied Research). Temperature control was maintained by using a jacketed cuvette holder coupled to a circulating temperature controlled water bath. High-pressure flash photolysis studies were carried out using a modified Nova Swiss pressure cell (Model 545.0040, three sapphire optical windows, 400 MPa max pressure) as described previously.^{17,18}

Spectrophotometric Titrations. UV–visible absorption spectra were recorded on a Cary 118 spectrophotometer with an OLIS upgrade computer interface. The sample solutions were first degassed by undergoing four fpt cycles and were then exposed to NO at various pressures and allowed to equilibrate for 45 min at 25 °C before recording the spectrum. NO pressure was measured with a mercury manometer and corrected for solvent vapor pressure.

Results

Spectrophotometric Titrations. The equilibrium constant for nitric oxide binding to **IIa** (eq 2) was determined by addition of NO to degassed solutions in acidic aqueous solution. The electronic spectra showed a decrease in absorbance at 396 nm with a concomitant increase at 426 nm (Figure 1). A Scatchard plot of the resulting data at 396 nm gives $K_{\text{eq}} = 4.9 \pm 0.1 \times 10^3 \text{ M}^{-1}$. The equilibrium constant for NO binding to **Ia** was



previously found to be $1.1 \times 10^3 \text{ M}^{-1}$ by similar methods.^{11a}

(17) (a) Crane, D. R.; Ford, P. C. *J. Am. Chem. Soc.* **1991**, *113*, 8510–8516. (b) Traylor, T. G.; Luo, J.; Simon, J. A.; Ford, P. C. *J. Am. Chem. Soc.* **1992**, *114*, 4340–4345.

(18) Crane, D. R.; Ford, P. C. *J. Am. Chem. Soc.* **1990**, *112*, 6871–6875.

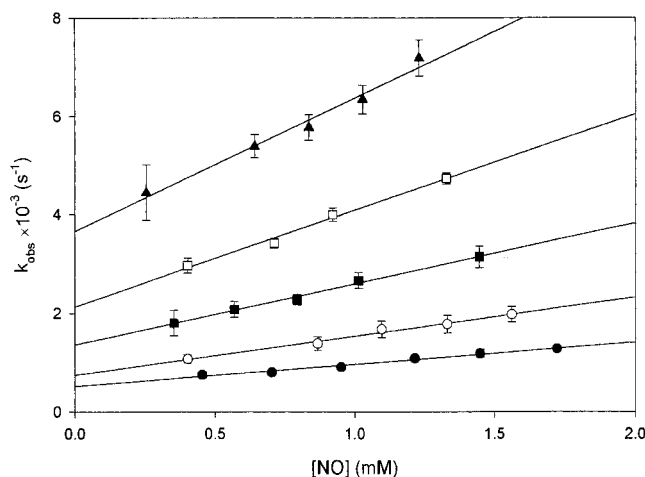
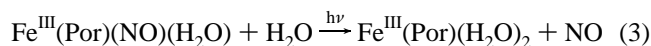


Figure 2. Plots of k_{obs} vs $[\text{NO}]$ for the reaction of NO with $\text{Fe}^{\text{III}}(\text{TPPS})$ as a function of temperature. (Filled circles = 25 °C, open circles = 30 °C, filled squares = 35 °C, open squares = 40 °C, triangles = 45 °C.)

Temperature and Pressure Effects on the Flash Photolysis Kinetics of $\text{Fe}^{\text{III}}(\text{Por})(\text{NO})$. When solutions of **Ia** and **IIa** were subjected to flash photolysis ($\lambda_{\text{ex}} = 355$ nm), the resulting transient difference spectra (Supporting Information Figure S-1) were consistent with the spectral differences between $\text{Fe}^{\text{III}}(\text{Por})(\text{NO})(\text{H}_2\text{O})$ and $\text{Fe}^{\text{III}}(\text{Por})(\text{H}_2\text{O})_2$ indicating that the photoreaction is simple displacement of the NO ligand (eq 3).



The spectral changes decayed exponentially in the presence of excess NO to give the initial equilibrium mixture of solvated and nitrosylated porphyrins. No permanent photoproducts were observed. The decay thus represents the relaxation back to equilibrium conditions. Accordingly, a plot of k_{obs} versus $[\text{NO}]$ should give a straight line with a slope equal to the rate constant for formation of the nitrosyl species (k_{on}) and an intercept equal to the rate constant for the reverse process (k_{off}) (eq 4).

$$k_{\text{obs}} = k_{\text{on}}[\text{NO}] + k_{\text{off}} \quad (4)$$

In this manner, the k_{on} values for **Ia** and **IIa** at 25 °C were found to be $(4.5 \pm 0.3) \times 10^5$ and $(2.8 \pm 0.2) \times 10^6 \text{ M}^{-1} \text{ s}^{-1}$, and k_{off} values of 500 ± 40 and $900 \pm 200 \text{ s}^{-1}$ were determined, respectively. The $k_{\text{on}}/k_{\text{off}}$ ratios give the values for the equilibrium constants for NO binding to **Ia** and **IIa** of $(1.0 \pm 0.1) \times 10^3$ and $(3.1 \pm 0.7) \times 10^3$, respectively. The first of these values is close to the equilibrium constant determined under steady-state conditions; the latter appears to be about 30% low.

Temperature effects on the reaction of NO with **Ia** and **IIa** were evaluated over the range 25–45 °C. Plots of k_{obs} versus $[\text{NO}]$ were linear at all temperatures (e.g., Figure 2 and Supporting Information Figure S-2), and the resulting k_{on} and k_{off} values are summarized in Table 1. Eyring plots of these data were found to be linear allowing for the determination of activation parameters ΔH^\ddagger and ΔS^\ddagger for both the “on” and “off” reactions. From these plots, enthalpies of activation for **Ia** and **IIa** were found to be 69 ± 3 and $57 \pm 3 \text{ kJ mol}^{-1}$ for the “on” reaction and 76 ± 6 and $84 \pm 3 \text{ kJ mol}^{-1}$ for the “off” reaction, respectively. The ΔS^\ddagger values for **Ia** and **IIa** were determined as 95 ± 10 and $69 \pm 11 \text{ J mol}^{-1} \text{ K}^{-1}$ for the “on” reaction and 60 ± 11 and $94 \pm 10 \text{ J mol}^{-1} \text{ K}^{-1}$ for the “off” reaction, respectively.

Table 1. Rate Constants for the “On” and “Off” Reaction of NO with $\text{Fe}^{\text{III}}(\text{Por})$ over the Temperature Range 25–45 °C in Acidic Aqueous Solution

T (°C)	$\text{Fe}^{\text{III}}(\text{TPPS}) + \text{NO}$		$\text{Fe}^{\text{III}}(\text{TMPS}) + \text{NO}$	
	k_{on} ($10^6 \text{ M}^{-1} \text{ s}^{-1}$)	k_{off} (10^3 s^{-1})	k_{on} ($10^6 \text{ M}^{-1} \text{ s}^{-1}$)	k_{off} (10^3 s^{-1})
25	0.5 ± 0.03	0.5 ± 0.4	2.8 ± 0.2	0.9 ± 0.2
30	0.8 ± 0.5	0.7 ± 0.6	4.5 ± 0.6	1.5 ± 0.1
35	1.2 ± 0.6	1.4 ± 0.5	6.4 ± 0.3	2.9 ± 0.3
40	2.0 ± 1.4	2.1 ± 0.1	9.9 ± 0.3	4.5 ± 0.4
45	2.7 ± 0.2	3.7 ± 0.2	13.0 ± 0.5	8.5 ± 0.4

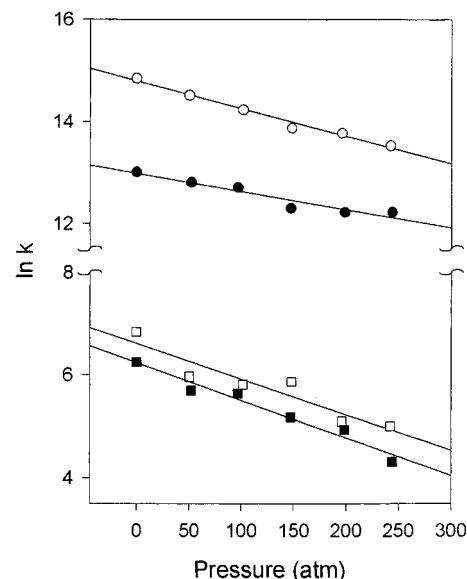


Figure 3. Plots of $\ln k_i$ vs P for the on (circles) and off (squares) reactions of NO with $\text{Fe}^{\text{III}}(\text{TPPS})$ (filled symbols) and $\text{Fe}^{\text{III}}(\text{TMPS})$ (open symbols).

The effects of hydrostatic pressure (P) on the kinetics of the reactions of **Ia** and **IIa** with NO were examined over the pressure range 0.1–250 MPa. Plots of k_{obs} versus $[\text{NO}]$ were linear at each pressure (Supporting Information Figure S-3), and from these plots, the values of k_{on} and k_{off} at various P values were determined. Plots of $\ln k_i$ versus P were linear (Figure 3) in accord with the first-order definition of the activation volume (eq 5). From the slopes of these plots, the $\Delta V_{\text{on}}^\ddagger$ values were

$$\Delta V_i^\ddagger = -RT \left[\frac{d \ln k_i}{dP} \right]_T \quad (5)$$

determined to be 9 ± 1 and $13 \pm 1 \text{ cm}^3 \text{ mol}^{-1}$ for k_{on} , while the $\Delta V_{\text{off}}^\ddagger$ values were found to be 18 ± 2 and $17 \pm 3 \text{ cm}^3 \text{ mol}^{-1}$ for **Ia** and **IIa**, respectively, at 25 °C.

Temperature and Pressure Effects on the Flash Photolysis Kinetics $\text{Fe}^{\text{II}}(\text{Por})(\text{NO})$. Flash photolysis ($\lambda_{\text{ex}} = 355$ nm) of **IIb(NO)** in 50 mM pH 7.0 phosphate buffer solution resulted in a transient absorbance spectrum equivalent to the difference spectrum generated by subtracting the steady-state spectra of **IIb** and **IIb(NO)** (Figure 4). The transient spectrum decayed exponentially back to the original spectrum with no observable permanent photoproducts. According to eq 4, plots of $[\text{NO}]$ versus k_{obs} were linear with slopes equal to k'_{on} (Supporting Information Figures S-4 and S-5). Notably, these values are about 3 orders of magnitude greater than those seen for the ferric analogues (Table 1 and Table 2) under analogous conditions. The intercepts of such plots should equal k'_{off} , but the equilib-

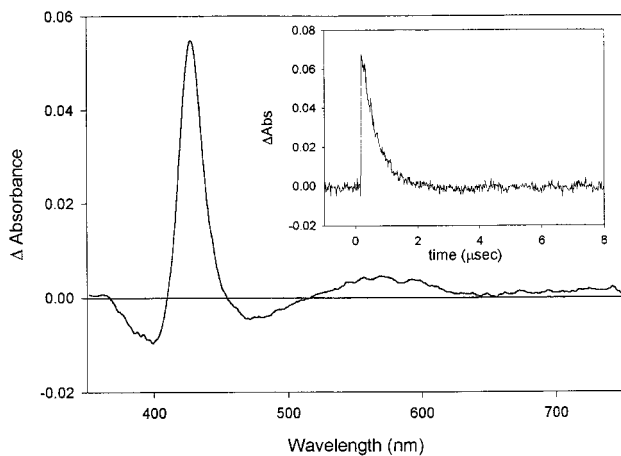
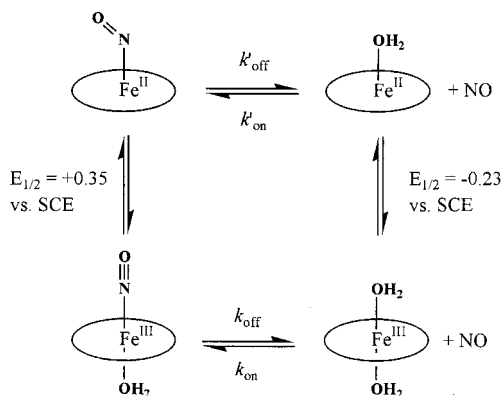


Figure 4. Transient difference spectrum of $\text{Fe}^{\text{II}}(\text{TMPS})\text{NO}$ under 1 atm of NO recorded by a CCD camera 50 ns after 355 nm flash photolysis. Inset: Temporal profile of the relaxation back to equilibrium recorded at 426 nm ($k_{\text{obs}} = 2.0 \times 10^6 \text{ s}^{-1}$).

Table 2. Rate Constants for the “On” Reaction of NO with $\text{Fe}^{\text{II}}(\text{Por})$ over the Temperature Range 25–45 °C in 50 mM pH 7.0 Phosphate Buffer

T (°C)	$\text{Fe}^{\text{II}}(\text{TPPS}) + \text{NO}$	$\text{Fe}^{\text{II}}(\text{TMPS}) + \text{NO}$
	$k_{\text{on}} (10^9 \text{ M}^{-1} \text{ s}^{-1})$	$k_{\text{on}} (10^9 \text{ M}^{-1} \text{ s}^{-1})$
25	1.5 ± 0.1	1.0 ± 0.01
30	1.9 ± 0.1	1.7 ± 0.04
35	2.0 ± 0.03	1.8 ± 0.1
40	2.6 ± 0.1	2.1 ± 0.04
45	2.9 ± 0.1	2.3 ± 0.1

Scheme 1. Born–Haber Cycle for Estimating the Value for the k_{off} Rate Constant¹⁹



rium constants for $\text{Fe}^{\text{II}}(\text{Por})(\text{NO})$ formation are so large that k_{off} values could not be accurately determined by extrapolation. However, a Born–Haber type cycle can be used to estimate the dissociation rate constant ($k'_{\text{off}} = 2 \times 10^{-4} \text{ s}^{-1}$) from electrochemical and kinetics data (Scheme 1).¹⁹ The equilibrium constant for NO binding to $\text{Fe}^{\text{II}}(\text{Por})$ is thus estimated to be $\sim 10^{12} \text{ M}^{-1}$ from these data (see later). Similar analysis has been used to determine equilibrium constants for NO binding to nitroporins.²⁰

(19) (a) $E_{1/2}$ for $\text{Fe}^{\text{III}}(\text{Por})\text{NO} = +0.35 \text{ V}$ vs SCE; $E_{1/2}$ for $\text{Fe}^{\text{III}}(\text{Por}) = -0.23 \text{ V}$ vs SCE. The value for k'_{off} was determined using the following expression:

$$k'_{\text{off}} = \frac{k_{\text{on}}}{K_{\text{NO}} e^{(nF\Delta E)/RT}}$$

where $k'_{\text{on}} = 1.5 \times 10^9 \text{ M}^{-1} \text{ s}^{-1}$ and $K_{\text{NO}} = 1.1 \times 10^3 \text{ M}^{-1}$. (b) Barley, M. H.; Meyer, T. J. *J. Am. Chem. Soc.* **1986**, *108*, 5876–85.

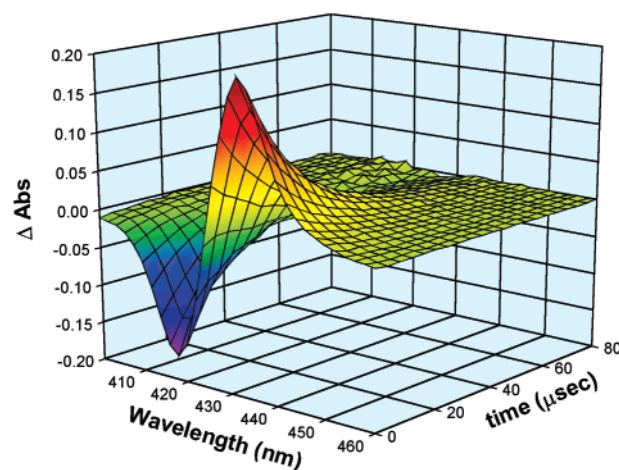


Figure 5. Transient absorbance spectrum in the Soret band region of aqueous $\text{Fe}^{\text{II}}(\text{TMPS})(\text{CO})$ under 1 atm of CO at 25 °C. The relaxation back to baseline occurred with an observed rate constant of $5.8 \pm 0.1 \times 10^4 \text{ s}^{-1}$.

The k_{on} values for the reactions of NO with **Ib** and **IIb** were determined over the temperature range 25–45° C from linear plots of k_{obs} versus $[\text{NO}]$ at each temperature (Table 2). Linear Eyring plots of these data gave values for $\Delta H_{\text{on}}^{\ddagger}$ and $\Delta S_{\text{on}}^{\ddagger}$ of $24 \pm 3 \text{ kJ mol}^{-1}$ and $12 \pm 10 \text{ J mol}^{-1} \text{ K}^{-1}$ for **Ib** and $26 \pm 6 \text{ kJ mol}^{-1}$ and $16 \pm 21 \text{ J mol}^{-1} \text{ K}^{-1}$ for **IIb**.

The hydrostatic pressure effects on the k_{on} values for the reaction of NO with **Ib** and **IIb** were examined over the pressure range 0.1–250 MPa. The k_{on} at each P was obtained from plots of k_{obs} versus $[\text{NO}]$. Plots of $\ln k_i$ versus P (Supporting Information Figures S-6 and S-7) gave $\Delta V_{\text{on}}^{\ddagger}$ values of 5 ± 1 and $2 \pm 2 \text{ cm}^3 \text{ mol}^{-1}$ for **Ib** and **IIb**, respectively, at 25° C.²¹

Temperature and Pressure Effects on the Flash Photolysis Kinetics of $\text{Fe}^{\text{II}}(\text{Por})(\text{CO})$. The temperature and hydrostatic pressure effects on the reaction of CO with **Ib** and **IIb** were examined by laser flash photolysis ($\lambda_{\text{ex}} = 355 \text{ nm}$) of solutions of these complexes in the presence of CO at various concentrations over the temperature range 25–45 °C and the pressure range 0.1–250 MPa. Flash photolysis of **Ib(CO)** and **IIb(CO)** solutions resulted in transient absorbance spectra consistent with photolabilization of CO followed by relaxation back to equilibrium conditions. In the presence of excess CO, the decay was monoexponential at all wavelengths (e.g., Figure 5). No permanent photoproducts were observed. Plots of k_{obs} versus $[\text{CO}]$ were linear at each temperature and pressure, allowing for the k_{on} rate constants to be determined as a function of temperature and pressure. The k_{off} values were too small to be meaningfully determined by this technique (Supporting Information Figures S-8 and S-9). The k_{on} values at 25 °C were $3.6 \pm 0.3 \times 10^7$ and $6.0 \pm 0.2 \times 10^7 \text{ M}^{-1} \text{ s}^{-1}$ for **Ib** and **IIb**, respectively. Table 3 lists the k_{on} values for **Ib** and **IIb** at various temperatures. Eyring plots were found to be linear and gave the $\Delta H_{\text{on}}^{\ddagger}$ values for the forward binding reaction of

(20) Andersen, J. F.; Ding, X. D.; Balfour, C.; Shokhireva, T. K.; Champagne, D. E.; Walker, F. A.; Montfort, W. R. *Biochemistry* **2000**, *39*, 10118–10131.

(21) (a) A referee has pointed out that the K_a of phosphate is pressure dependent, thus changing the pH of the buffer solution as a function of pressure, and that this may influence the measured ΔV^{\ddagger} values. However, experiments were conducted in pH 6.0 phosphate buffer that gave results that were in agreement with those conducted at pH 7.0. The change in K_a for phosphate would result in a solution with a pH of ~ 6 at the highest pressure in this study. (b) Larson, J. W.; Zeeb, K. G.; Hepler, L. G. *Can. J. Chem.* **1982**, *60*, 2141–2150.

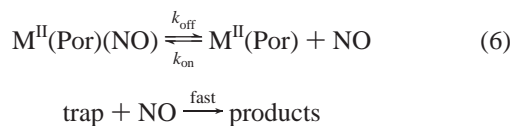
Table 3. Rate Constants for the “On” Reaction of CO with Fe^{II}(Por) and for the Reaction of NO with Co^{II}(TPPS) over the Temperature Range 25–45 °C in 50 mM pH 7.0 Phosphate Buffer

<i>T</i> (°C)	Fe ^{II} (TPPS) + CO	Fe ^{II} (TMPS) + CO	Co ^{II} (TPPS) + NO
	k_{on} (10 ⁷ M ⁻¹ s ⁻¹)	k_{on} (10 ⁷ M ⁻¹ s ⁻¹)	k_{on} (10 ⁹ M ⁻¹ s ⁻¹)
25	3.6 ± 0.3	6.0 ± 0.2	1.9 ± 0.3
30	3.9 ± 0.1	6.8 ± 0.2	2.5 ± 0.1
35	4.2 ± 0.1	8.9 ± 0.2	2.9 ± 0.02
40	4.6 ± 0.2	11.0 ± 0.1	3.3 ± 0.1
45	5.1 ± 0.1	13.5 ± 0.4	4.3 ± 0.1

11 ± 6 and 31 ± 4 kJ mol⁻¹ and the Δ*S*_{on}[‡] values of -64 ± 2 and 6 ± 13 J mol⁻¹ K⁻¹ for **Ib** and **IIb**, respectively. Values of *k*_{on} for the pressure dependent studies were determined from rates measured at three [CO] at different hydrostatic pressures (Supporting Information Figure S-10). Plots of ln *k*_{on} versus *P* were linear, giving Δ*V*[‡] values of -6 ± 0.6 and -4.0 ± 0.7 cm³ mol⁻¹ for **Ib** and **IIb**, respectively, at 25 °C. Notably, Δ*V*_{on}[‡] values for CO are *negative* in sharp contrast to *positive* values determined for the reactions with NO.

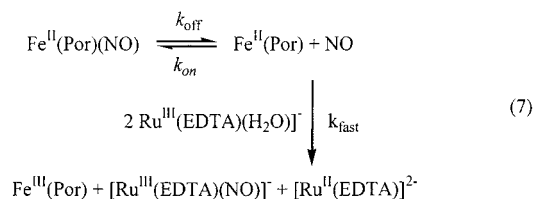
Temperature Effects on the Flash Photolysis Kinetics of Co^{II}(TPPS)(NO). Temperature effects on the reaction of NO with **IIIb** were examined by laser flash photolysis (λ_{ex} = 355 nm) over the temperature range 25–45 °C. The transient absorbance spectrum recorded 50 ns after the laser flash was consistent with photolabilization of NO. Temporal spectral changes indicated relaxation back to equilibrium conditions, because no permanent photoproducts were observed. Plots of *k*_{obs} versus [NO] were linear, allowing for the determination of *k*_{on} from the slope of these plots (Supporting Information Figure S-10); however, the intercepts were too small to allow the determination of *k*_{off} with reasonable certainty. The second-order rate constant *k*_{on} at 25 °C was found to be 1.9 ± 0.3 × 10⁹ M⁻¹ s⁻¹. Eyring plots for the *k*_{on} values at different *T* (Table 3) were linear, allowing for the determination of Δ*H*_{on}[‡] and Δ*S*_{on}[‡] as 28 ± 2 kJ mol⁻¹ and 26 ± 7 J mol⁻¹ K⁻¹, respectively.

NO Dissociation Rates from Fe^{II}(TPPS)(NO) and Co^{II}(TPPS)(NO). The rate of NO dissociation from Fe^{II}(TPPS)(NO) was estimated according to Scheme 1¹⁹ to be ~2 × 10⁻⁴ s⁻¹, a value too small to be determined by extrapolation in laser flash photolysis studies. However, the dissociation rates may be measured by using a trapping agent according to eq 6. Although dithionite anion reacts rapidly with NO,²² preliminary studies suggest that dithionite also influences the NO dissociation



rate from Fe^{II}(TPPS)(NO), and, hence, is not a suitable trapping agent in this case.²³ An alternative is [Ru^{III}(EDTA)(H₂O)]⁻, which traps NO with a rate constant of 2.24 × 10⁷ M⁻¹ s⁻¹ in pH 7.4 aqueous solution at 7 °C.²⁴ Because [Ru^{III}(EDTA)(H₂O)]⁻ is capable of oxidizing Fe^{II}(TPPS) to Fe^{III}(TPPS) but does not interact with Fe^{II}(TPPS)(NO), the overall reaction scheme is that shown in eq 7, the rate-limiting step being *k*_{off}. Solutions of Fe^{II}(TPPS)(NO) were prepared as before, NO was removed by rapid evacuation, and excess

[Ru^{III}(EDTA)(H₂O)]⁻ in degassed buffer solution was added. The observed first-order rate constant for formation of Fe^{III}(TPPS)(H₂O)₂ was found to be 6.3 × 10⁻⁴ s⁻¹, about three times higher than that estimated from Scheme 1. However, given the uncertainties in the electrochemical data used in that estimate, the agreement is reasonable.

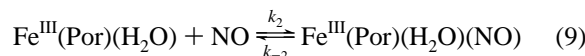
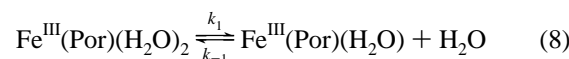


Similar experiments using [Ru^{III}(EDTA)(H₂O)]⁻ as a trapping agent were conducted with Co^{II}(TPPS)(NO) leading to the formation of Co^{III}(TPPS). The value of *k*_{off} thus measured is 1.5 × 10⁻⁴ s⁻¹ at 25 °C.

The equilibrium constants (*K*) for M^{II}(Por)(NO) complex formation can be calculated from the ratio of *k*_{on} (determined by flash photolysis experiments) to *k*_{off} (determined by trapping experiments). These *k*_{on}/*k*_{off} ratios are 2.4 × 10¹² M⁻¹ and 1.3 × 10¹³ M⁻¹ for Fe^{II}(TPPS) and Co^{II}(TPPS), respectively.

Discussion

Reactions of the Fe(III) Complexes. The large and positive values of Δ*S*_{on}[‡] and Δ*V*_{on}[‡] for *k*_{on} and *k*_{off} for the reaction of NO with the Fe^{III}(Por) complexes **Ia** and **IIa** are signatures for ligand substitution dominated by ligand dissociation, for example,



Consistent with a dissociative mechanism is the report by Hunt et al. that H₂O exchange between solvent and Fe^{III}(TPPS)(H₂O)₂³⁻ occurs at a first-order rate (*k*_{ex} = 1.4 × 10⁷ s⁻¹ in 25 °C water), far exceeding the *k*_{obs} values determined under any [NO] studied here.²⁵ Taking the steady-state approximation with regard to the unsaturated intermediate Fe^{III}(Por)(H₂O), the expression describing *k*_{obs} for relaxation to equilibrium following flash photolysis would be

$$k_{\text{obs}} = \frac{k_1 k_2 [\text{NO}] + k_{-1} k_{-2} [\text{H}_2\text{O}]}{k_{-1} [\text{H}_2\text{O}] + k_2 [\text{NO}]} \quad (10)$$

Under the experimental conditions, it is reasonable to conclude that *k*₋₁[H₂O] ≫ *k*₂[NO], because both *k*₋₁ and *k*₂ involve the trapping of an unsaturated metal center and [H₂O] ≫ [NO]. Thus, the expression for *k*_{obs} takes the form

$$k_{\text{obs}} = \frac{k_1 k_2 [\text{NO}]}{k_{-1} [\text{H}_2\text{O}]} + k_{-2} \quad (11)$$

Accordingly, *k*_{on} = *k*₁*k*₂/*k*₋₁[H₂O], and *k*_{off} = *k*₋₂.

In this context, Δ*V*_{on}[‡] = Δ*V*₁[‡] + Δ*V*₂[‡] - Δ*V*₋₁[‡], and Δ*S*_{on}[‡] = Δ*S*₁[‡] + Δ*S*₂[‡] - Δ*S*₋₁[‡]. Because the *k*₂ and *k*₋₁ steps represent similar (very fast) reactions of the unsaturated intermediate with a small neutral ligand (NO or H₂O, respectively), the differences in their activation volumes and entropies should be small (i.e.,

(22) Moore, E. G.; Gibson, Q. H. *J. Biol. Chem.* **1976**, *251*, 2788–94.

(23) Laverman, L. E. Unpublished data.

(24) Davies, N. A.; Wilson, M. T.; Slade, E.; Fricker, S. P.; Murrer, B. A.; Powell, N. A.; Henderson, G. R. *Chem. Commun.* **1997**, 47–48.

(25) Ostrich, I. J.; Gordon, L.; Dodgen, H. W.; Hunt, J. P. *Inorg. Chem.* **1980**, *19*, 619.

Table 4. Activation Parameters for the “On” and “Off” Reactions of NO and CO with the Water Soluble Metalloporphyrin Systems Described in This Study

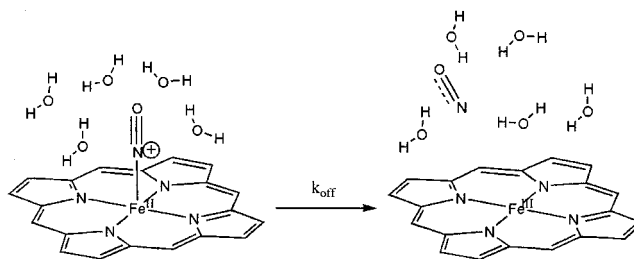
reaction	k (25 °C)	ΔH^\ddagger (kJ mol ⁻¹)	ΔS^\ddagger (J mol ⁻¹ K ⁻¹)	ΔV^\ddagger (cm ³ mol ⁻¹)
“on” reactions (M ⁻¹ s ⁻¹)				
Fe ^{III} (TPPS) + NO	4.5 × 10 ⁵	69 ± 3	95 ± 10	9 ± 1
Fe ^{III} (TMPS) + NO	2.8 × 10 ⁶	57 ± 3	69 ± 11	13 ± 1
Fe ^{II} (TPPS) + NO	1.5 × 10 ⁹	24 ± 3	12 ± 10	5 ± 1
Fe ^{II} (TMPS) + NO	1.0 × 10 ⁹	26 ± 6	16 ± 21	2 ± 2
Fe ^{II} (TPPS) + CO	3.6 × 10 ⁷	11 ± 6	-64 ± 2	-6.6 ± 0.6
Fe ^{II} (TMPS) + CO	6.0 × 10 ⁷	31 ± 4	6 ± 13	-4.0 ± 0.7
Co ^{II} (TPPS) + NO	1.9 × 10 ⁹	28 ± 2	26 ± 7	<i>a</i>
“off” reactions (s ⁻¹)				
Fe ^{III} (TPPS)(NO)	500	76 ± 6	60 ± 11	18 ± 2
Fe ^{III} (TMPS)(NO)	900	84 ± 3	94 ± 10	17 ± 3

^a Not determined.

$\Delta V_2^\ddagger - \Delta V_{-1}^\ddagger \approx 0$ and $\Delta S_2^\ddagger - \Delta S_{-1}^\ddagger \approx 0$). In that case, the “on” reaction is dominated by k_1 , the dissociation of H₂O to form the unsaturated intermediate. Therefore, $\Delta H_{\text{on}}^\ddagger$ should largely reflect the energy required to break the Fe^{III}-OH₂ bond, while the positive $\Delta S_{\text{on}}^\ddagger$ and $\Delta V_{\text{on}}^\ddagger$ values are consistent with formation of two species from one without charge creation.

A dissociative mechanism requires that H₂O exchange proceeds by a comparable pathway. In this context, the activation parameters reported by Hunt et al. for the exchange of H₂O coordinated to **Ia** ($\Delta H_{\text{ex}}^\ddagger = 57$ kJ mol⁻¹ and $\Delta S_{\text{ex}}^\ddagger = 84$ J mol⁻¹ K⁻¹) are in reasonable agreement with those reported here for k_{on} .²⁵ A recent study by van Eldik et al. using variable temperature/pressure NMR techniques reports $\Delta H_{\text{ex}}^\ddagger = 67$ kJ mol⁻¹, $\Delta S_{\text{ex}}^\ddagger = 99$ J mol⁻¹ K⁻¹, and $\Delta V_{\text{ex}}^\ddagger = 7.9$ cm³ mol⁻¹ for **Ia**, in even better agreement with those shown in Table 4 for the k_{on} pathway of **Ia** with NO.²⁶ Thus, the factors that determine the exchange kinetics for the Fe(III) diaquo species **Ia** with solvent H₂O dominate the kinetics for NO reaction with the same species, that is, the k_{on} activation parameters for **Ia** and **IIa** are largely defined by the dissociative mechanism, with the limiting step being eq 6.

The principle of microscopic reversibility argues that the intermediate(s) in the reverse reaction (k_{off}) will be the same intermediates as those generated during the k_{on} pathway. For k_{off} , the energetically dominant k_{-2} step involves breaking the iron nitrosyl bond. Coordination of NO to Fe^{III}(Por) is accompanied by considerable charge transfer to give a linearly bonded diamagnetic {Fe^{II}(NO)}⁶ complex which can be formally represented as Fe^{II}(Por)-(NO⁺).^{27,28} Thus, the activation parameters of the “off” reaction reflect the intrinsic entropy and volume changes associated with the spin change and solvent reorganization as the charge redistributes, as illustrated in Figure 6. The large positive $\Delta V_{\text{off}}^\ddagger$ values for **Ia** and **IIa** are consistent with the limiting dissociative mechanism as outlined in eqs 8 and 9. The specific solvation of the NO coordinated to Fe(III) and the resulting solvent reorganization upon NO dissociation (Figure 6) have some analogy in the NO carrying nitrophorins. The crystal structure of one nitrophorin, NP4, shows that binding of NO to the Fe(III) center leads to a collapse of the protein

**Figure 6.** Schematic representation of the solvent reorganization that occurs upon the loss of nitric oxide from Fe^{III}(Por) in aqueous solution. (The Fe^{III}(Por)(NO) complex is represented as having charge transfer to the metal (Fe^{II}(Por)(NO⁺)) consistent with the linear NO structure observed in similar porphyrins by X-ray crystallography).²⁴**Table 5.** Rate Constants for the “On” and “Off” Rates of Ferri- and Ferro-Heme Proteins

ferric proteins ^a	k_{on} (M ⁻¹ s ⁻¹)	k_{off} (s ⁻¹)	ref
eNOS ^b	6.1 × 10 ⁵	93	25
eNOS ^c	8.2 × 10 ⁵	70	25
eNOS ^d	2.8 × 10 ⁵	100	25
nNOS ^e	2.1 × 10 ⁷	40	26
nNOS ^f	6.0 × 10 ⁶	70	26
mMb ^g	4.8 × 10 ⁴	43	12
mMb ^h	1.9 × 10 ⁵	13.6	11a
NP ⁱ	1.5–2.2 × 10 ⁶	0.006–2.2	20
mCyt ^j	7.2 × 10 ²	4.4 × 10 ⁻²	11a
Cat ^k	3.0 × 10 ⁷	170	11a
ferrous proteins ^a	k_{on} (M ⁻¹ s ⁻¹)	k_{off} (s ⁻¹)	ref
eNOS ^b	1.1 × 10 ⁶	45	25
eNOS ^c	1.1 × 10 ⁶	70	25
eNOS ^d	8.9 × 10 ⁵	50	25
nNOS ^e	1.1 × 10 ⁷	~0	26
nNOS ^f	9.8 × 10 ⁶	~0	26
SGC ^l	1.4 × 10 ⁸		35
SGC ^m		6–8 × 10 ⁻⁴	40
SGC ⁿ		5.0 × 10 ⁻²	40
Mb ^o	1.7 × 10 ⁷	1.2 × 10 ⁻⁴	35
Hb ₄ ^{T,p}	2.6 × 10 ⁷	3.0 × 10 ⁻³	43
Hb ₄ ^{R,p}	2.6 × 10 ⁷	1.5 × 10 ⁻⁴	43
Cyt ^j	8.3	2.9 × 10 ⁻⁵	11a

^a eNOS = endothelial nitric oxide synthase, nNOS = neuronal nitric oxide synthase, Mb = myoglobin, NP = nitrophorin, Cyt = cytochrome *c*, Cat = catalase, sGC = soluble guanylyl cyclase. ^b 10 °C. ^c 10 °C in the presence of 1 mM arginine. ^d 10 °C in the presence of 1 mM *N*-hydroxy arginine. ^e pH 7.8, 20 °C, heme domain. ^f pH 7.8, 20 °C, holoenzyme. ^g Horse heart myoglobin, 50 mM phosphate buffer, pH 7.0, 25 °C. ^h Aqueous solution of sperm whale skeletal myoglobin. ⁱ Reported rate constants are the range for NP1, NP2, NP3, and NP4, pH 5.0 and pH 8.0, 25 °C; the dissociation process k_{off} displays two phases. ^j Aqueous solution of horse heart cytochrome *c*. ^k Aqueous solution of bovine liver catalase. ^l Two phases are observed for NO binding. ^m pH 7.4, 20 °C. ⁿ pH 7.4, 20 °C in the presence of 3 mM Mg²⁺ and 0.5 mM GTP. ^o As quoted in ref 35 from Eich, R. F. Ph.D. Dissertation, Rice University, Houston, TX, 1997. ^p pH 7.0, 20 °C.

around the coordinated NO. The distal heme binding pocket in NP4 is quite open to solvent in the absence of NO. It was postulated that the collapse of the protein around the heme nitrosyl led to increased retention of bound NO at low pH.²⁰

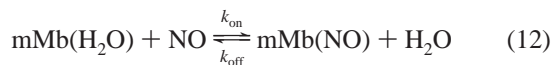
The k_{on} (25 °C) values have been reported earlier by Hoshino et al. for the analogous reaction of NO with the ferri-heme proteins met-myoglobin (mMb, $k_{\text{on}} = 1.9 \times 10^5$ M⁻¹ s⁻¹), catalase ($k_{\text{on}} = 3.0 \times 10^7$ M⁻¹ s⁻¹), and ferri-cytochrome *c* ($k_{\text{on}} = 7.2 \times 10^2$ M⁻¹ s⁻¹) (Table 5).^{11a} The nearly 5 orders of magnitude differences in these values can be attributed to the

(26) Schnepfensieper, T.; Zahl, A.; van Eldik, R. *Angew. Chem.* **2001**, *40*, 1678–1680.

(27) (a) Enemark, J. H.; Feltham, R. D. *Coord. Chem. Rev.* **1974**, *13*, 339–406. (b) Wayland, B. B.; Newman, A. R. In *Diatom Molecular Complexes of Metalloporphyrins*; Longo, F. R., Ed.; Ann Arbor Science: Ann Arbor, MI, 1979.

(28) Scheidt, W. R.; Gouterman, M. In *Iron Porphyrins Pt I*; Lever, A. B. P., Gray, H. B., Eds.; Addison-Wesley Publishing: London, 1983.

differences in protein structure. For catalase and mMb, the entering NO ligand displaces a water molecule (eq 12), as is the case with the model systems described here. However, ferri-cytochrome *c* has a methionine sulfur as well as a histidine nitrogen coordinated to the Fe(III) metal center.



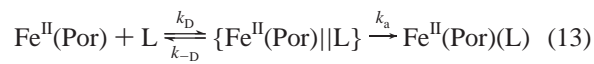
Studies in this laboratory in collaboration with the laboratories of van Eldik and Stochel¹² determined activation parameters for reaction of NO with mMb according to eq 12. Values of $\Delta H_{\text{on}}^\ddagger = 63 \pm 2 \text{ kJ mol}^{-1}$, $\Delta S_{\text{on}}^\ddagger = 55 \pm 8 \text{ J mol}^{-1} \text{ K}^{-1}$, and $\Delta V_{\text{on}}^\ddagger = 20 \pm 6 \text{ cm}^3 \text{ mol}^{-1}$ as well as $\Delta H_{\text{off}}^\ddagger = 68 \pm 4 \text{ kJ mol}^{-1}$, $\Delta S_{\text{off}}^\ddagger = 14 \pm 13 \text{ J mol}^{-1} \text{ K}^{-1}$, and $\Delta V_{\text{off}}^\ddagger = 18 \pm 3 \text{ cm}^3 \text{ mol}^{-1}$ were determined, respectively. Comparison of these activation parameters with those determined for reactions of NO with **Ia** and **IIa** demonstrate that these compounds are reasonable models, at least for this ferri-heme protein.

Other ferri-heme proteins for which k_{on} and k_{off} values have been reported include two forms of nitric oxide synthase eNOS²⁹ and nNOS³⁰ as well as several forms of nitrophorin.²⁰ With the exception of ferri-cytochrome *c*, which is structurally quite different from the other proteins (see previously), the “on” and “off” rates are similar for the various ferri-heme proteins. As noted above, release of NO from the nitrophorins requires considerable protein reorganization induced by increases in pH and histamine concentration. The requisite rearrangement is apparently the cause of the somewhat slower “off” rates for the various NP’s.

Reactions of the Fe(II) Complexes. The “on” rates for reaction of NO with the ferrous complexes **Ib** and **IIb** are about 3 orders of magnitude larger than those for the iron(III) analogues. Correspondingly, the activation parameters demonstrate much lower values of $\Delta H_{\text{on}}^\ddagger$ and $\Delta S_{\text{on}}^\ddagger$. The magnitude of the latter is consistent with rates largely defined by diffusional factors,³¹ although the k_{on} values reported for **Ib** and **IIb** are nearly an order of magnitude less than diffusion limits in water.³² High spin Fe^{II}(Por) complexes are considerably more labile than the Fe^{III}(Por) analogues. Because the heme may be 5-coordinate, NO may form a metal–NO bond without first displacing another ligand. Ferro-heme proteins also have been shown to have widely varying k_{on} values with NO, presumably because of structural differences. Hemoglobin ($k_{\text{on}} = 2.7 \times 10^7 \text{ M}^{-1} \text{ s}^{-1}$, 25 °C) and myoglobin ($k_{\text{on}} = 1.7 \times 10^7 \text{ M}^{-1} \text{ s}^{-1}$), both of which have 5-coordinate Fe^{II} centers, react rapidly with NO.³³ However, the reaction with ferro-cytochrome *c* ($8.3 \text{ M}^{-1} \text{ s}^{-1}$)^{11a} is many orders of magnitude slower. Like ferri-cytochrome *c*, ferro-cytochrome *c* is hexacoordinate with histidine and methionine ligands in the axial heme sites. The low reactivity of both forms of cytochrome *c* are consistent with the substitution mechanism proposed above for the ferri-heme complexes.

Previous kinetics studies³⁴ of ferro-heme proteins and model compounds have led to a suggested mechanism in which an

encounter complex, {Fe^{II}(Por)||L}, is formed prior to ligand bond formation according to



where k_D is the rate constant for the diffusion-limited formation of the encounter complex, k_{-D} is the rate constant for diffusion apart, and k_a is that for the “activation” step, M–L bond formation. On the basis of the steady-state approximation for the encounter complex, the apparent rate constant for the “on” reaction is

$$k_{\text{on}} = \frac{k_D k_a}{k_{-D} + k_a} \quad (14)$$

and the activation volume is defined as

$$\Delta V_{\text{on}}^\ddagger = \Delta V_D^\ddagger + \Delta V_a^\ddagger - RT \left(\frac{d \ln(k_a + k_{-D})}{dP} \right) \quad (15)$$

This scheme has two limiting cases, one in which the reaction is diffusion limited ($k_a \gg k_{-D}$) and the other in which the reaction is activation limited ($k_{-D} \gg k_a$). In the activation limited process, eq 15 simplifies to

$$\Delta V_{\text{on}}^\ddagger = \Delta V_D^\ddagger + \Delta V_a^\ddagger - \Delta V_{-D}^\ddagger \quad (16)$$

where $\Delta V_D^\ddagger - \Delta V_{-D}^\ddagger$ is the volume difference between the encounter complex and the solvent separated species. Although unknown, this is likely to be small for a small neutral ligand such as NO, because the encounter complex does not involve the formation or breaking of bonds and should have only a modest impact on solvation. The dominant term would be ΔV_a^\ddagger , which should give negative contributions owing to Fe^{II}–L bond formation and the concomitant change of the spin state from high (quintet Fe^{II}(Por) plus doublet NO) to low spin (doublet Fe^{II}(Por)(NO)).³⁵

If $k_a \gg k_{-D}$, the reaction would be diffusion-limited, and eq 15 reduces to $\Delta V_{\text{on}}^\ddagger = \Delta V_D^\ddagger$. Activation volumes for diffusion in various solvents are positive owing to viscosity increases with increased pressure (+7.5, +9.5, and +0.8 cm³ mol⁻¹ in CH₃CN, EtOH, and H₂O respectively).³⁶ For **Ib** and **IIb**, the positive $\Delta V_{\text{on}}^\ddagger$ values are somewhat larger than would be expected for a diffusion limited process in aqueous solution but are significantly smaller than those measured for the iron(III) analogues. If the Fe^{II}(Por) are weakly hexacoordinate in aqueous solution, there may be a modest dissociative contribution to the activation volume. Regardless of this contribution, the reaction mechanism is clearly dominated by diffusional terms. Therefore, the pressure data are consistent with a process having a k_{on} value within an order of magnitude of the diffusion limit in water ($k_d \sim 10^{10} \text{ M}^{-1} \text{ s}^{-1}$ at 298 K).³⁷ If a similar analysis were made with respect to $\Delta S_{\text{on}}^\ddagger$, then $\Delta S_{\text{on}}^\ddagger = \Delta S_D^\ddagger$ in the diffusion-limited case. The activation entropy ΔS_D^\ddagger for diffusion of water in aqueous solution can be calculated as $\sim 34 \text{ J mol}^{-1} \text{ K}^{-1}$.³⁸ The measured $\Delta S_{\text{on}}^\ddagger$ for **Ib** and **IIb** (12 ± 10 and $16 \pm 21 \text{ J mol}^{-1} \text{ K}^{-1}$, respectively) are thus consistent with a process largely

(29) Abu-Soud, H. M.; Ichimori, K.; Presta, A.; Stuehr, D. J. *J. Biol. Chem.* **2000**, *275*, 17349–17357.

(30) Scheele, J. S.; Bruner, E.; Kharitonov, V. G.; Martásek, P.; Roman, L. J.; Masters, B. S.; Sharma, V. S.; Magde, D. *J. Biol. Chem.* **1999**, *274*, 13105–13110.

(31) Caldin, E. F. In *Fast Reactions in Solution*; J. Wiley and Sons: New York, 1964; p 12.

(32) Turley, W. D.; Offen, H. W. *J. Phys. Chem.* **1984**, *88*, 3605.

(33) Moore, E. G.; Gibson, Q. H. *J. Biol. Chem.* **1976**, *251*, 2788–2794.

(34) Rose, E. J.; Hoffman, B. M. *J. Am. Chem. Soc.* **1983**, *105*, 2866–73.

(35) DiBenedetto, J. D.; Arkle, V.; Goodwin, H. A.; Ford, P. C. *Inorg. Chem.* **1985**, *24*, 455–456.

(36) Turley, W. D.; Offen, H. W. *J. Phys. Chem.* **1984**, *88*, 3605–3606.

(37) Caldin, E. In *Fast Reactions in Solution*; Wiley and Sons: New York, 1964.

(38) Glasstone, S.; Laidler, K. J.; Eyring, H. In *The Theory of Rate Processes*; McGraw-Hill: New York, 1941.

limited by diffusion. Similar arguments can be made for the reaction of NO with $\text{Co}^{\text{II}}(\text{TPPS})$.

In order for nitric oxide to act as an intracellular signaling agent at submicromolar concentrations, the reactions with ferrohemes must be very fast to compete with other chemical and physiological processes leading to NO depletion. This study is consistent with the intuitive notion that the fast reactions of ferro-heme proteins with NO are due to a vacant or exceedingly labile coordination site. In this context, very large k_{on} values have long been known for reaction of NO with hemoglobin ($1.4 \times 10^7 \text{ M}^{-1} \text{ s}^{-1}$) and myoglobin ($1.7 \times 10^7 \text{ M}^{-1} \text{ s}^{-1}$) and have recently reported for guanylyl cyclase ($1.4 \times 10^8 \text{ M}^{-1} \text{ s}^{-1}$).³⁹

The model proposed in eq 13 and subsequent analysis for the reaction of NO with $\text{Fe}^{\text{II}}(\text{Por})$ applies to the analogous reactions with CO. The second-order rate constants for the reaction of **Ib** and **IIb** with CO are several orders of magnitude below the diffusion limit, and as a consequence, this reaction must be activation limited. In contrast to the reaction with NO, the $\Delta V_{\text{on}}^{\ddagger}$ values for CO are negative. These results parallel other studies of ferro-heme complexes that found reaction with NO to be diffusion limited, while reaction with CO is activation limited.¹⁷ This model was confirmed by a study of the reaction of CO with $\text{Fe}^{\text{II}}(\text{MCPH})$ (MCPH = monochelated protoheme, protohemin 3-(1-imadazoyl) propylamine stearyl ester) in toluene/mineral oil solutions, where it was shown by exploiting pressure effects that the reaction could be tuned from being activation limited to being diffusion limited.^{17b} The change in mechanism occurred because of increased solvent viscosity as a function of hydrostatic pressure, making the diffusion rate, k_{D} , much slower.

The quantum yields for photodissociation of NO or CO from the isoelectronic $\{\text{M}-\text{XY}\}^6$ systems $\text{Fe}^{\text{III}}(\text{Por})(\text{NO})$, $\text{Fe}^{\text{II}}(\text{Por})(\text{CO})$, and $\text{Mn}^{\text{II}}(\text{Por})(\text{NO})$ are near unity while those for $\text{Fe}^{\text{II}}(\text{Por})(\text{NO})$ are generally quite small when measured by nanosecond flash photolysis methods.⁴⁰ However, ultrafast flash techniques have shown that solvent caged pairs $\{\text{Fe}^{\text{II}}(\text{Por})\|\text{NO}\}$ are formed in high yields even for the $\text{Fe}^{\text{II}}(\text{Por})(\text{NO})$ systems.^{10g} These caged pairs, although prepared differently, are formally similar to the encounter complexes proposed in eq 11. While formed in high yields, these $\{\text{Fe}^{\text{II}}(\text{Por})\|\text{NO}\}$ caged pairs decay back to $\text{Fe}^{\text{II}}(\text{Por})(\text{NO})$ rapidly and efficiently (i.e., $k_{\text{a}} \gg k_{-\text{D}}$); hence, quantum yields for NO dissociation are very small. In contrast, the analogous encounter complex formed by flash photolysis of the $\text{Fe}^{\text{II}}(\text{Por})(\text{CO})$ analogue diffuses apart rapidly (i.e., $k_{\text{a}} \ll k_{-\text{D}}$). Therefore, the caged pairs formed by flash photolysis behave the same as the proposed encounter complex.

The differing behaviors of NO and CO in their reactions with $\text{Fe}^{\text{II}}(\text{Por})$ have been argued to be the result of different spin-orbit states in the encounter complex (or caged pair). For example, the reaction of high spin $\text{Fe}^{\text{II}}(\text{TPPS})$ ($S = 2$) with NO ($S = 1/2$) results in the formation of a low spin doublet species $\text{Fe}^{\text{II}}(\text{TPPS})(\text{NO})$ ($S = 1/2$). A similar spin change is seen for reaction of $\text{Co}^{\text{II}}(\text{TPPS})$ ($S = 3/2$) with NO ($S = 1/2$) to form $\text{Co}^{\text{II}}(\text{TPPS})(\text{NO})$ ($S = 0$). It has been hypothesized that the spin change may have an effect on the activation parameters for the reaction of NO with metalloporphyrin complexes.⁴¹ However, given the nearly diffusion limited reaction rates, contributions to the activation energies from spin state changes must be small.

(39) Sharma, V. S.; Magde, D. *Methods—Companion to Methods Enzymol.* **1999**, *19*, 494–505.

(40) (a) Hoffman, B. M.; Gibson, Q. H. *Proc. Natl. Acad. Sci.* **1978**, *75*, 21–25 and references therein. (b) Rose, E. J.; Hoffman, B. M. *J. Am. Chem. Soc.* **1983**, *105*, 2866–2873.

(41) Chernoff, D. A.; Hochstrasser, R. M.; Steele, A. W. *Proc. Nat. Acad. Sci.* **1980**, *77*, 5606–5610.

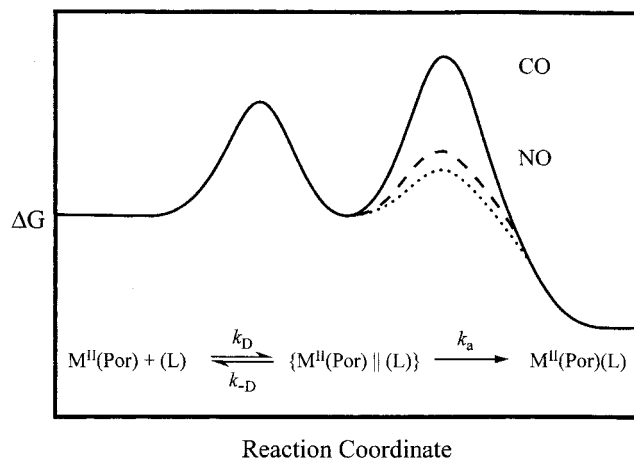


Figure 7. Schematic energy diagram illustrating the barriers from diffusion (k_{D}) and activation (k_{a}). The reactions of $\text{Fe}^{\text{II}}(\text{Por})$ with CO (solid line) and NO (dashed line) illustrate a change in mechanism from activation limited to diffusion limited, respectively. The reaction of NO with $\text{Co}^{\text{II}}(\text{Por})$ (dotted line) is similarly diffusion limited.

There is clearly a much greater barrier to CO recombination from a caged pair (or encounter complex) with $\text{Fe}^{\text{II}}(\text{Por})$ than for the analogous reactions with NO. This has been represented in earlier discussions in terms of an activation barrier for the reaction with CO, while the barrier for NO is much smaller or nonexistent, as shown schematically in Figure 7.⁴² Harvey has recently confirmed the validity of the barrier for CO binding by DFT calculations,⁴³ but similar calculations have not been carried out for NO.

The k_{off} for $\text{Fe}^{\text{II}}(\text{TPPS})(\text{NO})$ was too small to measure by flash photolysis techniques. However, the thermodynamic cycle described in Scheme 1 allows estimating k_{off} having a value of $2 \times 10^{-4} \text{ s}^{-1}$, while direct measurements using $[\text{Ru}^{\text{III}}(\text{EDTA})(\text{H}_2\text{O})]^-$ as a trapping agent gave $k_{\text{off}} = 6 \times 10^{-4}$. Similar low values have been estimated and/or measured for other Fe^{II} porphyrins and ferro-heme nitrosyls confirming the very large equilibrium constant for $\text{Fe}^{\text{II}}(\text{Por})\text{NO}$ binding. Because the “off” reaction is crucial for the down regulation of sGC, it is notable that different values for k_{off} have been reported for this protein depending on reaction conditions. For example, k_{off} was measured by Kharitonov et al.⁴⁴ as $6\text{--}8 \times 10^{-4} \text{ s}^{-1}$ in pH 7.4 buffer solution (20 °C), but values several orders of magnitude higher ($5.0 \times 10^{-2} \text{ s}^{-1}$) were found in the presence of the enzyme substrates guanylyl triphosphate (GTP) and Mg^{2+} , and an even higher value has been reported for reactions in vivo (3.7 s^{-1} , 37 °C).⁴⁵ The coordination environment of Fe(II) in sGC largely determines the NO dissociation rates. The protein is activated 400-fold following NO binding leading to formation of pentacoordinate heme. It has been shown that coordination of proximal histidine to give 6-coordinate Fe(II) reduces the equilibrium constant for NO binding by a factor of 10^4 , with most of the decrease due to an increase in NO dissociation rate.³⁹ Bohle has reported the k_{off} rates from $\text{Fe}^{\text{II}}(\text{Por})(\text{NO})$ can be

(42) (a) Petrich, J. W.; Poyart, C.; Martin, J. L. *Biochemistry* **1988**, *27*, 4049–4060. (b) Cornelius, P. A.; Hochstrasser, R. M.; Steele, A. W. *J. Mol. Biol.* **1983**, *163*, 11–128. (c) Quillin, M. L.; Li, T.; Olson, J. S.; Phillips, G. N.; Dou, Y.; Ikeda-Saito, M.; Regan, R.; Carlson, M.; Gibson, Q. H.; Li, H.; Elber, R. *J. Mol. Biol.* **1995**, *245*, 416–436. (d) Carver, T. E.; Rohlfis, R. J.; Olson, J. S.; Gibson, Q. H.; Blackmore, R. S.; Springer, B. A.; Sligar, S. G. *J. Biol. Chem.* **1990**, *265*, 20007–20020.

(43) Harvey, J. N. *J. Am. Chem. Soc.* **2000**, *122*, 12401–12402.

(44) Kharitonov, V. G.; Russwurm, M.; Madge, D.; Sharma, V. S.; Koesling, D. *Biochem. Biophys. Res. Commun.* **1997**, *239*, 284–286.

(45) Bellamy, T. C.; Garthwaite, J. *J. Biol. Chem.* **2001**, *276*, 4287–4292.

manipulated by modifying the electronic/steric nature of the porphyrin and has noted that various ligands in solution can accelerate NO dissociation from $\text{Fe}^{\text{II}}(\text{TPPS})(\text{NO})$.^{10j,23}

Summary

Although lacking the detailed molecular polypeptide architectures, the water soluble Fe(II) and Fe(III) porphyrins display reactivity properties relevant to the mechanisms of NO reactions with ferro- and ferri-heme proteins with which NO plays biological roles. In many such proteins, one coordination site on the iron is accessible either because the metal is penta-coordinate or because the sixth coordination site is occupied by a labile H_2O ligand. The latter is the case for Fe(III) porphyrins, and kinetics of forming the metal–NO bond are governed by the lability of the leaving ligand; activation parameters indicate a dissociative mechanism for the “on” reaction (and for the microscopic reverse, the NO “off” reaction). Thus, for the ferri-heme complexes, the free radical nature of NO, which is of crucial importance to the physiological roles played by NO, appears to have only a minor influence on the ligand substitution dynamics.

In contrast, differences between NO and a 2-electron donor ligand such as CO are clearly apparent when one examines the reactivities with the pentacoordinate Fe(II) porphyrins. Because leaving group lability is no longer a determining factor, the reactions are orders of magnitude faster than with the Fe(III) analogues, consistent with the high reactivity required of the ferro-heme protein sGC in the bioregulatory action of sub-micromolar NO. Indeed, the reactions of NO with ferrous

porphyrins **Ib** and **IIb** and with $\text{Co}^{\text{II}}(\text{TPPS})$ approach diffusion limited rates, in contrast to much slower reactions with the Fe(III) analogues and of CO with the ferrous porphyrins. The difference between NO and CO in such reactions is apparently due to a greater activation barrier in forming the $\text{Fe}^{\text{II}}\text{--CO}$ bond from the $\{\text{Fe}^{\text{II}}(\text{Por})\|\text{CO}\}$ encounter complex (eq 13) than for the analogous bond formation from $\{\text{Fe}^{\text{II}}(\text{Por})\|\text{NO}\}$ or $\{\text{Co}^{\text{II}}(\text{Por})\|\text{NO}\}$. Difference in spin state changes appear to have similar contributions to the activation barriers in the reactions of NO with **Ib**, **IIb**, and $\text{Co}^{\text{II}}(\text{TPPS})$. Similar behavior has been observed for myoglobin,⁴⁶ and the lowered barrier in the relaxation of $\{\text{Fe}^{\text{II}}(\text{Por})\|\text{NO}\}$ to the bound form may be attributed to spin–orbit coupling of the NO and Fe^{II} electronic states as well as mixing of ground and low lying charge transfer states.⁴¹

Acknowledgment. These studies were supported by the National Science Foundation (CHE 9726889). We would like to thank Ivan Lorkovic for discussions of the Born–Haber cycle depicted in Scheme 1 used to estimate the “off” rates for $\text{Fe}^{\text{II}}(\text{TPPS})(\text{NO})$.

Supporting Information Available: Ten supplemental figures. This material is available free of charge via the Internet at <http://pubs.acs.org>.

JA0113910

(46) (a) Olson, J. S.; Phillips, G. N. *J. Biol. Chem.* **1996**, *271*, 17593–17596. (b) Ikeda-Saito, M.; Dou, Y.; Yonetani, T.; Olson, J. S.; Li, T.; Regan, R.; Gibson, Q. H. *J. Biol. Chem.* **1993**, *268*, 6855–6857.